Ligand−Integrin $\alpha_V\beta_3$ Interaction Determined by Photoaffinity Cross-Linking: A Challenge to the Prevailing Model†

Gal Bitan,§ Lukas Scheibler,§ Dale F. Mierke,‡ Michael Rosenblatt,§ and Michael Chorev*,§

Division of Bone and Mineral Metabolism, Charles A. Dana and Thorndike Laboratories, Department of Medicine, Beth Israel Deaconess Medical Center, 330 Brookline Avenue, Boston, Massachusetts 02215 and Department of Molecular Pharmacology, Physiology, & Biotechnology, Division of Biology and Medicine, Brown University, Providence, Rhode Island 02912

Received April 18, 2000; Revised Manuscript Received June 7, 2000

ABSTRACT: Integrin $\alpha_V\beta_3$ plays a crucial role in angiogenesis, apoptosis, and bone remodeling, mainly by interacting with matrix proteins through recognition of an Arg−Gly−Asp (RGD) motif. Recently, a small cyclic RGD-containing $\alpha_V\beta_3$-ligand possessing a C-terminal photoreactive group was photo-cross-linked within β_3[99−118], in the N-terminus of the β_3 chain [Bitan G et al. (1999) *Biochemistry* 38, 3414−3420]. In this paper, a photoreactive group at the N-terminus of the RGD-ligand is shown to interact within β_3[167−171], approximately 60 residues C-terminal to the previously identified domain. On the basis of these findings, a model of the putative I-like domain of the β_3 subunit, homologous to α_M-, α_L-, and α_2-I-domains, reveals that the β_3[99−118] and β_3[167−171] contact sites are close to each other and are on the opposite side relative to the metal ion-dependent adhesion site (MIDAS) motif. These observations contradict the prevailing model that proposes proximity between metal- and RGD-binding sites on the I-like domain. Our data suggest that either the I-like domain structure predicted for β_3 is incorrect, or there is no spatial proximity between the RGD-binding site and the MIDAS motif in the I-like domain. Our results indicate that the current models for ligand−receptor interaction should be revisited.

Integrins are cell membrane-bound heterodimeric receptors able to transduce signals between the extracellular environment and the cytoplasm (*1*). They participate in cell extracellular matrix (ECM)[1] and cell−cell adhesion (*2*, *3*) and are involved in fundamental cellular processes such as migration, proliferation, and survival (*4*). The family of integrins currently consists of 23 known receptors, each composed of an α- and a β-subunit, which play a crucial role not only in normal physiology but also in many pathological conditions, such as metastasis of malignancies (*5*).

The interaction of integrins with their endogenous ligands is often based on recognition of short peptide motifs in the ligands. The most common motif is the arginyl−glycyl−aspartyl (RGD) sequence (*6*). This triad is also the major binding determinant in disintegrins, which are small proteins found in snake and other animal venoms. Disintegrins, as well as many synthetic RGD-based peptides (*7*, *8*), peptidomimetics (*9*), and non-peptides (*10*) have been shown to act as heterologous ligands for specific integrins both in vitro (*11*) and in vivo (*12*, *13*).

All integrins bind ligands in a divalent metal ion (Ca^{2+}/Mg^{2+})-dependent manner. The role of the metal cations has been shown to be complex, and the mechanism of metal-dependent binding is not completely understood. In some cases, Ca^{2+} is necessary for ligand binding, yet in other cases it has been shown to have an inhibitory effect (*14*−*16*).

The α- and the β-subunits share the same overall structure: a large N-terminal extracellular component, a transmembrane domain, and a short C-terminal intracellular tail. The physicochemical properties of integrins, being large heterodimeric transmembrane receptors, preclude direct structural investigations of the whole molecule by currently available high-resolution methods such as X-ray crystallography or NMR. Nevertheless, a wealth of structural data has been generated indirectly by lower-resolution methods, such as mutational analysis (*17*−*22*), creation of receptor chimeras (*23*−*26*) and deletion-containing mutants (*27*, *28*), biological characterization of peptides derived from putative binding sites (*29*, *30*), and generation of activating (*31*, *32*) or inhibitory (*29*, *33*−*35*) antibodies. Additionally, direct lower-resolution approaches have been utilized to investigate integrin-ligand interactions by chemical (*36*, *37*) and photoaffinity (*38*−*42*) cross-linking.

† This work was supported in part by Grant AR42833 (to M.R.) from the National Institute of Arthritis and Musculoskeletal Disease, National Institutes of Health.

* To whom correspondence should be addressed: Dr. Michael Chorev, Beth Israel Deaconess Medical Center, 330 Brookline Ave. (HIM 944), Boston, MA 02215. Telephone: 617-667-0901. Fax: 617-667-4432. E-mail: michael_chorev@hms.harvard.edu.

§ Beth Israel Deaconess Medical Center.

‡ Brown University.

[1] Abbreviations: Ahx, 6-aminohexanoyl; BH, Bolton−Hunter group; Bp, benzophenone; Bpa, L-4-benzoylphenylalanine; Dmt, L-5,5-dimethylthiazolidinecarboxylic acid; ECM, extracellular matrix; Endo-F, endoglycosidase-F/N-glycosidase F; Glu-C, endoproteinase Glu-C; HEK, human embryonic kidney; IEF, isoelectric focusing; Lys-C, lysyl endopeptidase; MIDAS, metal ion-dependent adhesion site; pBz_2, *p*-benzoylbenzoyl; PBS, phosphate-buffered saline; TLCK, 1-chloro-3-tosylamido-7-amino-2-heptanone; vWF, von Willebrand factor.

10.1021/bi000877a CCC: $19.00
Published on Web 08/12/2000

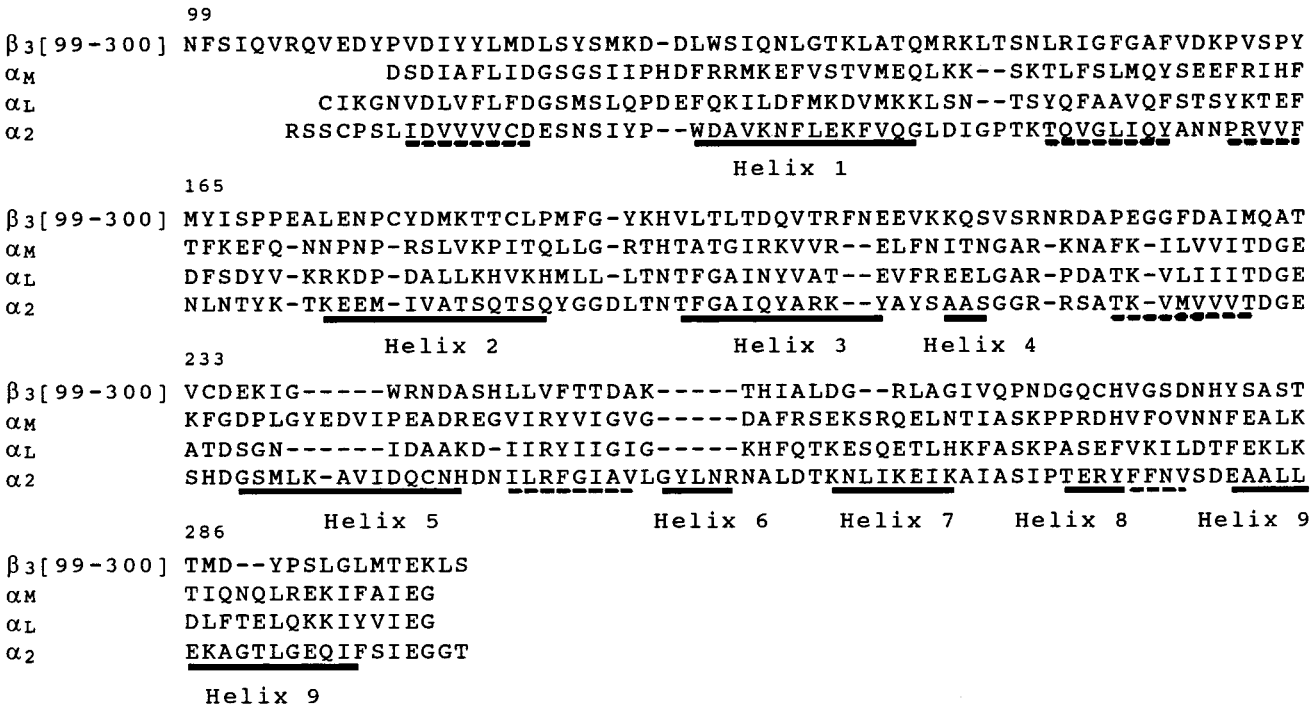

FIGURE 1: Sequence alignment of β_3[99−300] and the I-domains from α_M, α_L, and α_2. Alignment was performed using ClustalW. Secondary structure found in the crystal structures of the three I-domains are indicated (solid lines, α-helices (numbered); dashed lines, β-strands).

To date the only high-resolution experimental structural data available for integrins come from X-ray crystallographic analyses of I-domains, which are inserted modules found at the N-terminal part of certain α-subunits (*43*−*50*). On the basis of homology modeling, other domains have been postulated, such as an I-like domain predicted in all β-subunits (*45*, *51*, *52*), a seven-blade β-propeller structure hypothesized at the N-terminus of α-subunits (*53*), and the recently suggested PSI domain at the N-terminus of β-subunits (*54*).

I-domains have been shown in several cases to contain the principal ligand-binding site (*55*). Within the I-domain, a metal ion-dependent adhesion site (MIDAS) motif provides oxygen-containing side chains that coordinate a metal cation, known to be essential for ligand binding (*55*). This noncontiguous motif is composed of a primary consensus sequence, DXSXS, and two additional secondary sites, all located at the apex of the I-domain module (*55*). Binding of the cation and the ligand are known to influence each other. For a long time, it has been unclear whether a direct interaction between the two components takes place in the bound state or whether "cross-talk" between cation and ligand is mediated indirectly through allosteric conformational rearrangements of the integrin molecule (*29*, *31*, *56*, *57*). A recent crystal structure of the α_2-I-domain complexed with a non-RGD, collagen-based ligand (*50*) reveals that the ligand interacts directly with the metal. Ligand binding causes a conformational rearrangement of the I-domain, which is mediated through a reorganization of the metal coordination by the MIDAS motif. However, whether this finding represents a general mechanism and can be extrapolated to RGD-based ligands and to the putative I-like domains is yet to be determined.

Integrin $\alpha_V\beta_3$ (vitronectin receptor) binds various RGD-containing proteins, including fibronectin, fibrinogen, vitronectin, von Willebrand factor (vWF), bone sialoprotein, and osteopontin (*58*). It plays a major role in physiological processes, such as angiogenesis (*59*−*61*), apoptosis (*1*, *62*, *63*), and bone resorption (*12*, *64*, *65*). $\alpha_V\beta_3$ is the most abundant integrin displayed by osteoclasts, the multinucleated cells exclusively responsible for bone resorption. The adhesion between the osteoclast and the extracellular bone matrix is mediated by $\alpha_V\beta_3$ and is believed to form the cell matrix "tight seal" that is essential for bone resorption to proceed (*58*, *66*). Therefore, inhibition of $\alpha_V\beta_3$ function provides a novel mechanism-based approach for treatment of diseases associated with increased bone resorption, such as osteoporosis (*12*, *13*) and hypercalcemia of malignancy (*67*). Rational design of inhibitors for $\alpha_V\beta_3$ will benefit considerably from elucidating the structural basis for interaction in the ligand−$\alpha_V\beta_3$ bimolecular complex.

Recently, we reported the design and synthesis of novel benzophenone-containing, "tagged", RGD-based ligands as tools for photoaffinity mapping of the $\alpha_V\beta_3$−ligand interface (*68*). Using one of these ligands, *cyclo* ^{125}I-BH-Ahx-[Cys−Asn−Dmt−Arg−Gly−Asp−Cys]-Bpa-NH_2 (**1**, Figure 2), we identified a small "contact domain" in the β_3-subunit, β_3[99−118], which contains the cross-linking site for the C-terminal *p*-benzoylphenylalanine (Bpa) residue in **1** (*42*). As part of our continuing effort to generate a detailed topological map of the integrin-ligand interface, we now report the presence of a second small contact domain at a distinct site on the β_3 chain, identified by cross-linking the N-terminal benzophenone (Bp) group present in the closely related analogue, *cyclo* Bp-[Cys−Asn−Dmt−Arg−Gly−Asp−Cys]-Lys(N^{ϵ}-[^{125}I-BH-Ahx])-NH_2 (*68*) (**2**, Figure 2).

EXPERIMENTAL PROCEDURES

Radioreceptor Binding Assay. The affinity of the peptides for purified human integrin $\alpha_V\beta_3$ was measured in a radioreceptor competition assay with ^{125}I-echistatin as a tracer as described (*69*).

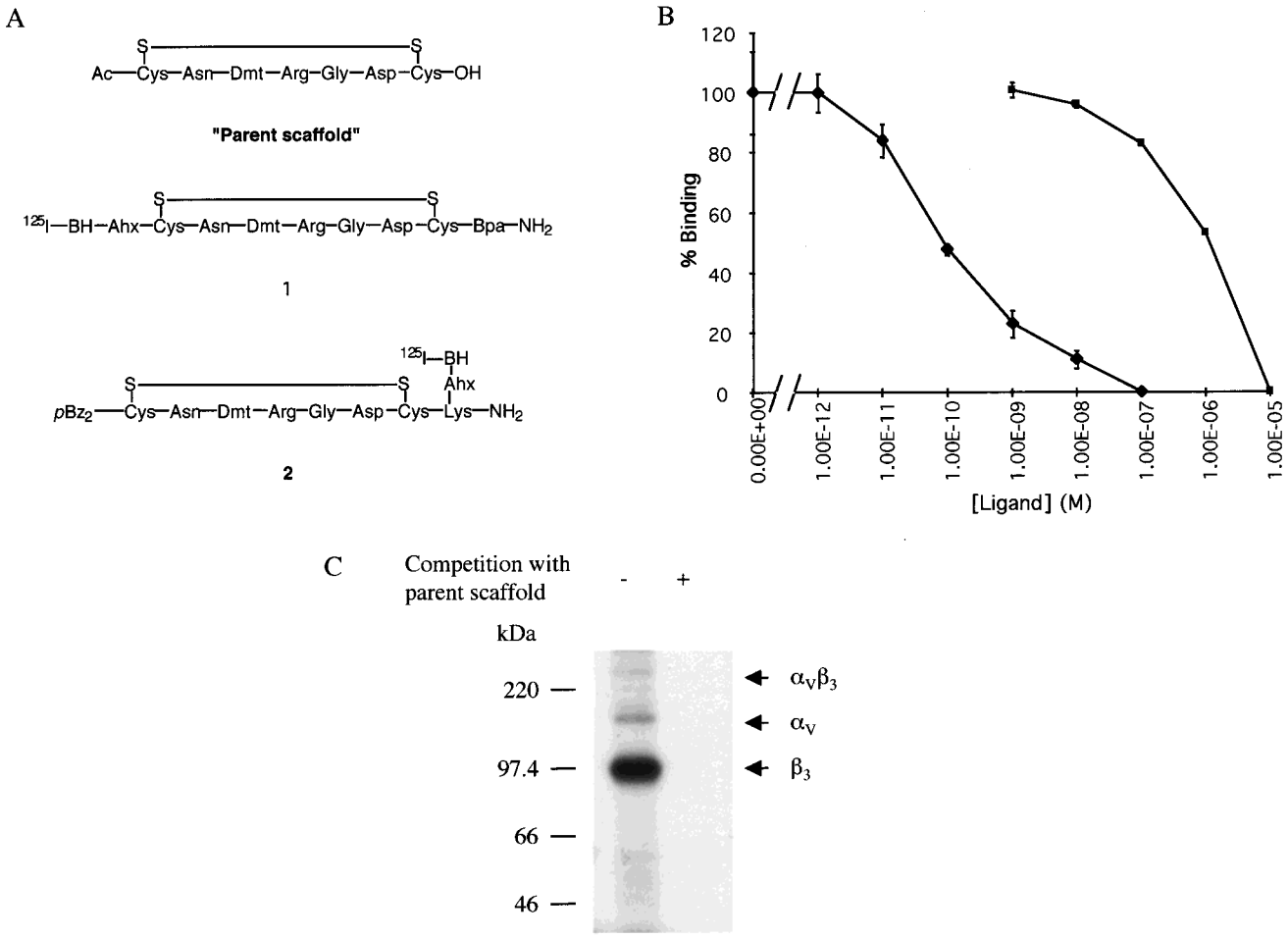

FIGURE 2: Characterization of ligand **2**. (A) Schematic structures of the parent scaffold and of ligands **1** and **2**. Ahx, 6-aminohexanoyl; Dmt, L-5,5-dimethylthiazolidine; Bpa, 4-benzoylphenylalanine; BH, Bolton−Hunter group. (B) Inhibition of binding of ^{125}I-echistatin to purified recombinant human $\alpha_V\beta_3$ by nonradioactive ^{127}I-**2** (■) and by nonradioactive echistatin (♦) as a standard. Results shown represent three independent experiments performed in triplicates. (C) Autoradiograph of photoaffinity cross-linking of **2** to $\alpha_V\beta_3$ expressed at ~10^6 copies/cell on HEK-293 cells, with and without competition by 10^{-5} M of the nonradioactive nonphotoreactive parent peptide, *cyclo* Ac-[Cys−Asn−Dmt−Arg−Gly−Asp−Cys]-OH. Samples were analyzed by 7.5% w/v SDS−PAGE. The main radioactive band at ~97 kDa corresponds to the β_3−**2** photoconjugate. The faint bands at ~150 and ~250 kDa correspond to radiolabeled α_V and nondenatured $\alpha_V\beta_3$ complex, respectively. Molecular weight markers are shown on the left side of the autoradiograph.

Introduction of ^{125}I-Bolton−Hunter Group. The unlabeled precursor of peptide **2** was labeled by coupling of an ^{125}I-Bolton−Hunter group (*70*) to the amino group of a 6-amino hexanoyl (Ahx) spacer attached to the side chain of Lys^8. The crude radiolabeled peptide **2** was purified by HPLC as described (*42*).

Photoaffinity Cross-Linking to HEK 293 Cells Overexpressing Integrin $\alpha_V\beta_3$. Radiolabeled peptide **2** (~7×10^8 cpm, ~160 pmol) was cross-linked to confluent HEK 293 cells stably expressing recombinant human integrin $\alpha_V\beta_3$ at ~10^6 copies/cell (10×75 cm^2 plates, ~9 nmol) according to a published protocol (*42*). Following cross-linking, the cells were washed 3 times with phosphate-buffered saline (PBS) and lysed by 30-min incubation with 10 mL of M-PER (Pierce, Rockford, IL). Cys residues were reduced and alkylated with iodoacetamide as previously reported (*71*), and the ligand−receptor photoconjugate was purified by preparative SDS−PAGE. The radioactivity of the gel band containing the β_3−**2** conjugate was ~$2-3 \times 10^6$ cpm, corresponding to 30−50% of the radioactivity loaded on the gel in different experiments. The photoconjugate was electroeluted from the gel with ~80% yield.

Enzymatic and Chemical Cleavage. Digestions of the β_3−**2** photoconjugate by endoglycosidase-F/N-glycosidase F (Endo-F), lysyl endopeptidase (Lys-C), BNPS-Skatole, and cyanogen bromide (CNBr) were performed as previously described (*71*). Chymotrypsin digestion was performed using 1-chloro-3-tosylamido-7-amino-2-heptanone (TLCK)-treated enzyme (Worthington Biochemical Co., Lakewood, NJ) to inhibit residual trypsin activity. A total of 50 μg of enzyme was used per reaction with 5000−30 000 cpm of the β_3−**2** photoconjugate. The digestion reaction was carried out in 100 μL volume of tris-buffer (25 mM tris-HCl, pH 8.5) at 37 °C overnight. Digestion with sequencing-grade endoproteinase Glu-C (Boehringer-Mannheim, Mannheim, Germany) was performed, after removal of SDS using SDS-Out (Pierce), by adding a small crystal of lyophilized enzyme to a 100-μL reaction containing 5000−30 000 cpm of the β_3−**2** photoconjugate in 25 mM $(NH_4)HCO_3$ buffer, pH 7.8. The reaction took place at room temperature overnight.

Isoelectric Focusing (IEF). Radioactive bands corresponding to CNBr-, Lys-C-, and chymotrypsin-generated β_3−**2** fragments were excised and electroeluted from 16.5% tricine/SDS gels in 1× SDS−PAGE running buffer. To eliminate

SDS, the samples were treated twice with SDS−Out and then dialyzed against 10 M urea overnight (*72*), followed by dialysis against ddH_2O for 24 h with five changes of ddH_2O. The SDS-free samples containing the radioactive fragments were concentrated by ultrafiltration on Microcon-3 devices (Amicon, Beverly, MA) (cutoff, 3000 Da) to 10−20 μL. The samples were analyzed on IEF Ready-Gels (Bio-Rad, Hercules, CA) with a pH gradient 3−10 using colored IEF protein standards (Bio-Rad). The radioactive bands were visualized by autoradiography.

Molecular Modeling. The molecular model of β_3[99−300] was built up using as templates the I-domain folds reported for α_2 (*43*), α_L (*44*), and α_M (*45*). The amino acid sequence of β_3[99−300] was constructed using a home-written distance geometry program and then fitted to the structural features of the I-domains using template-forcing applied during a short molecular dynamics simulation (simulated annealing) carried out using the CVFF91 force field within the Discover program (Molecular Simulations, Inc., San Diego, CA).

The atoms used for the template-forcing of β_3 to the I-domain structure were pulled from the sequence homology between β_3 and the α-subunit I-domains obtained from ClustalW as illustrated in Figure 1. Of the I-domains, two of the helical domains were not included in the fitting (helices 5 and 6, using the secondary structure nomenclature of α_2). The long helix 5 observed in α_2 is only a turn of a helix in α_L (four residues in length) and α_M (six residues in length) and represents a gap in the sequence in β_3 (Figure 1). Helix 6 of α_2 is a gap in the sequence for α_L, α_M, and β_3 and therefore was not used in the fitting.

All of the β-strands of the I-domains were used in the template-forcing procedure. For modeling of the N-terminus of the β_3 I-like domain, including residues β_3[99−112], the X-ray structure of vWF A1-domain (*73*), which is structurally defined in this region, was utilized.

The InsightII program (Molecular Simulations, Inc.) was used for all of the molecular modeling and producing of the figures. For comparison, the model of β_3 as proposed by Tozer et al. (*21*) was created using the template-forcing procedure, as described above but with application of the sequence homology as suggested in Figure 1 of Tozer et al. (*21*). To this model, we added the structural features of the N-terminus of the β_3 I-like domain, consisting of residues β_3[99−112], employing the vWF A1-domain structure as a template.

RESULTS

*Cross-Linking of Ligand **2** to Recombinant Human $\alpha_V\beta_3$ Stably Overexpressed in HEK 293 Cells.* Ligand **2** (Figure 2A) was prepared as part of a series of ligands based on the cyclic heptapeptide scaffold, *cyclo* Ac[Cys−Asn−Dmt−Arg−Gly−Asp−Cys]-OH (Figure 2) (*68*). The first ligand in this series, used for cross-linking studies (ligand **1**), incorporated a benzophenone photoprobe at its C-terminus and a radioiodine "tag" at the N-terminus (Figure 2A). Utilizing ligand **1**, we recently found that the C-terminus of the ligand cross-links to a site within the 20-amino acid sequence β_3[99−118], adjacent to the sequence $D^{119}LSYS^{123}$ in the MIDAS-like motif of β_3 (*42*). In ligand **2**, the photoprobe and the radioactive tag switch places relative to their positions in ligand **1**. Ligand **2** can be used to elucidate the contact site for the N-terminal part of the ligand. Ligand **2** binds human $\alpha_V\beta_3$ with an IC_{50} value of 1.0 ± 0.2 μM (Figure 2B).

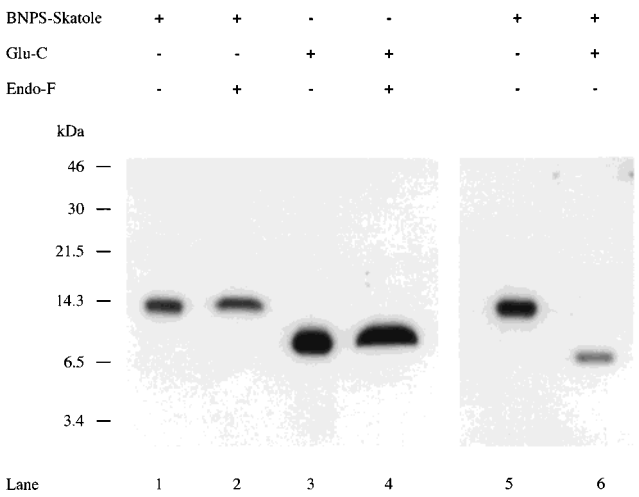

FIGURE 3: Digestions of the β_3−**2** photoconjugate by BNPS-Skatole (lanes 1 and 5) and Glu-C (lane 3). Lanes 2 and 4: treatment of the BNPS-Skatole- and Glu-C-generated bands, respectively, with Endo-F. Lane 6: treatment of the BNPS-Skatole-generated band with Glu-C. Samples were analyzed by 16.5% w/v Tricine/SDS−PAGE. This autoradiograph is a representative example of three reproducible independent experiments. Molecular weight markers are shown on the left side of the autoradiograph.

In all cross-linking experiments, the integrin/peptide ratio was maintained at ~50:1 to minimize nonspecific cross-linking. The complex was irradiated by UV light (365 nm) to form the photoconjugate, which was extracted from the cell membrane and analyzed by SDS−PAGE. Peptide **2** cross-linked specifically and efficiently to the $\alpha_V\beta_3$ receptor (Figure 2C). As previously observed for ligand **1**, cross-linking occurred predominantly to the β_3 chain, with less than 5% labeling of the α_V chain (Figure 2C). No cross-linking was observed in the presence of 10 μM of the parent scaffold (IC_{50} = 0.05 ± 0.02 μM) (Figure 2C) or with untransfected HEK 293 cells lacking $\alpha_V\beta_3$ (not shown).

Identification of the Contact Domain. The β_3−**2** photoconjugate was isolated by preparative SDS−PAGE and subjected to an array of enzymatic or chemical cleavages. Digestion with BNPS−Skatole, a reagent that specifically cleaves C-terminally to tryptophan residues, yielded a radiolabeled band with an apparent molecular mass of 14−15 kDa (Figure 3, lane 1). The theoretical BNPS−Skatole digestion map of the β_3 sequence (*74*) reveals two adjacent fragments located at the N-terminal part of the molecule consistent with the observed band: β_3[26−129] and β_3[130−238] (Figure 4A). One of these two fragments, β_3[26−129], is putatively glycosylated at Asn 99, whereas the β_3[130−238] fragment does not contain a consensus glycosylation site. To distinguish between these two possible cross-linking sites, we compared the apparent molecular masses of the BNPS−Skatole-generated fragment before and after treatment with Endo-F. Repeated treatment of the BNPS−Skatole-generated fragment with Endo-F in three independent experiments showed no difference between the apparent molecular masses of the radioactive band before and after the Endo-F reaction, suggesting that the cross-linking occurred within β_3[130−238] (Figure 3, compare lanes 1 and 2).

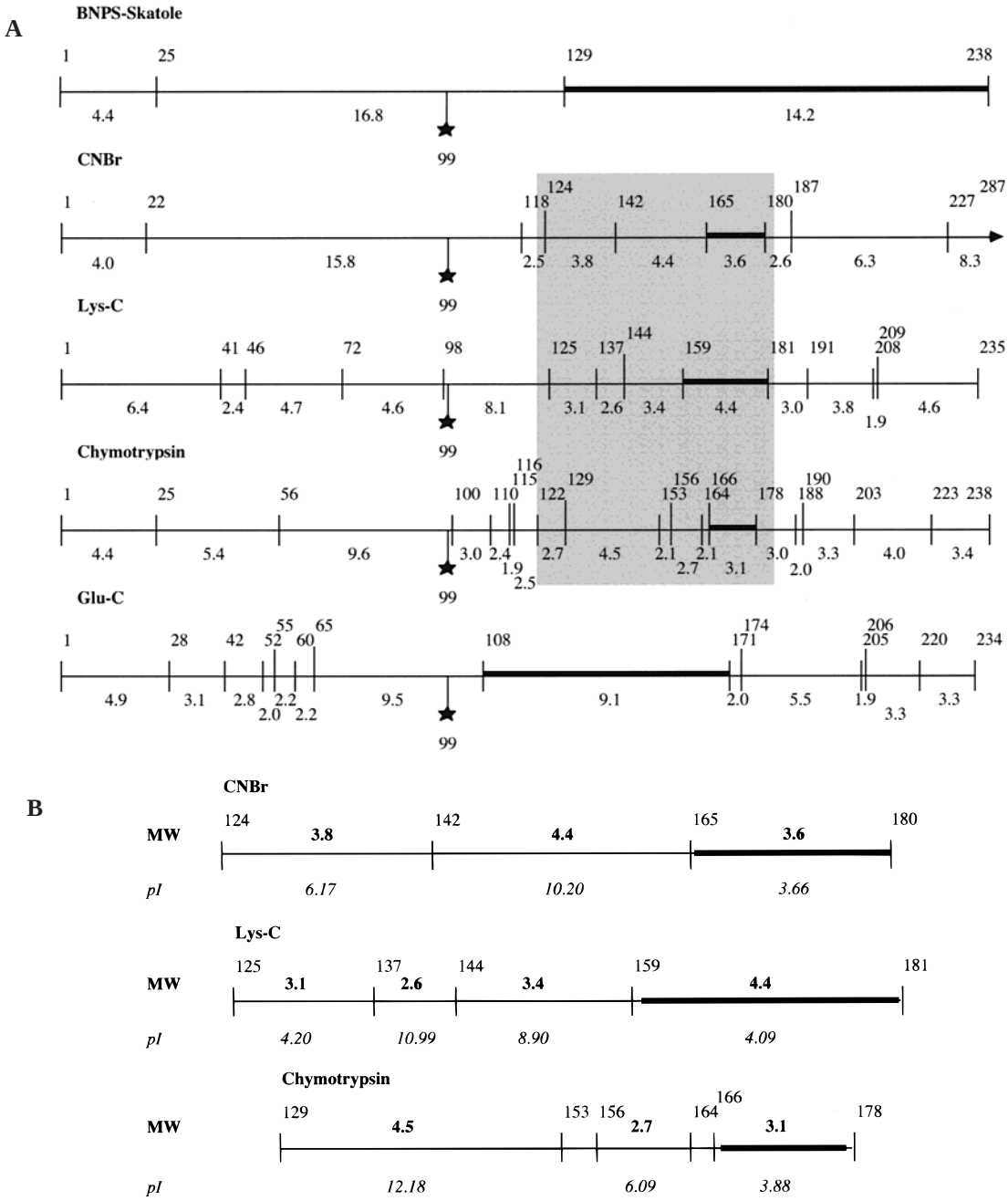

FIGURE 4: Theoretical digestion maps of the N-terminal third of the β_3 chain for the different cleavage agents used. Cleavage is always C-terminal to the indicated residue. Molecular mass (in kDa) indicated are of *S*-acetamido-alkylated fragments, glycosylated (if appropriate) and conjugated to the nondigestible ligand. (A) Cleavage points (upper numbers) are shown for endopeptidases Lys-C, chymotrypsin, and Glu-C, for the Met-specific reagent CNBr and for the Trp-specific reagent BNPS−Skatole. The lower numbers indicate the putative molecular masses. A bold line highlights the putative contact domain attributed to each cleavage pathway. A star represents a putative glycosylation site. The shaded area is enlarged in panel B. (B) Enlargement of the shaded area in panel A with indication of the predicted molecular mass in kDa (bold) above each fragment and the calculated p*I* value (italics) under the fragment. The p*I* values are given only for fragments in the appropriate molecular mass range (2.5−4.5 kDa) and are of the β_3 fragments conjugated to the ligand.

Further elucidation of the position of the contact site comes from treatment of the β_3−**2** photoconjugate with endoproteinase Glu-C, which yields a band with an apparent molecular mass of 9−10 kDa (Figure 3, lane 3). Under the conditions used for the Glu-C digestion (ammonium bicarbonate buffer, pH 7.8), this enzyme cleaves preferentially at the C-terminal side of glutamyl residues, as well as the peptide bond within Asp−Gly dipeptides. The theoretical digestion map shows three possible fragments corresponding to the observed Glu-C-generated band: two fragments at the N-terminal region, β_3[66−108] and β_3[109−171], the former of which is glycosylated at position 99 (Figure 4A), and one within the cysteine-rich domain, β_3[536−582], which is glycosylated at position 559 (not shown). Following the same rationale as discussed above for the BNPS−Skatole-generated fragment, similarity in the apparent molecular masses of the intact and Endo-F-treated Glu-C-generated bands in three independent experiments (Figure 3, compare lanes 3 and 4) indicates that the fragment β_3[109−171] contains the cross-linking site.

Combining the results from both BNPS−Skatole and Glu-C digestions reveals that the putative cross-linking site

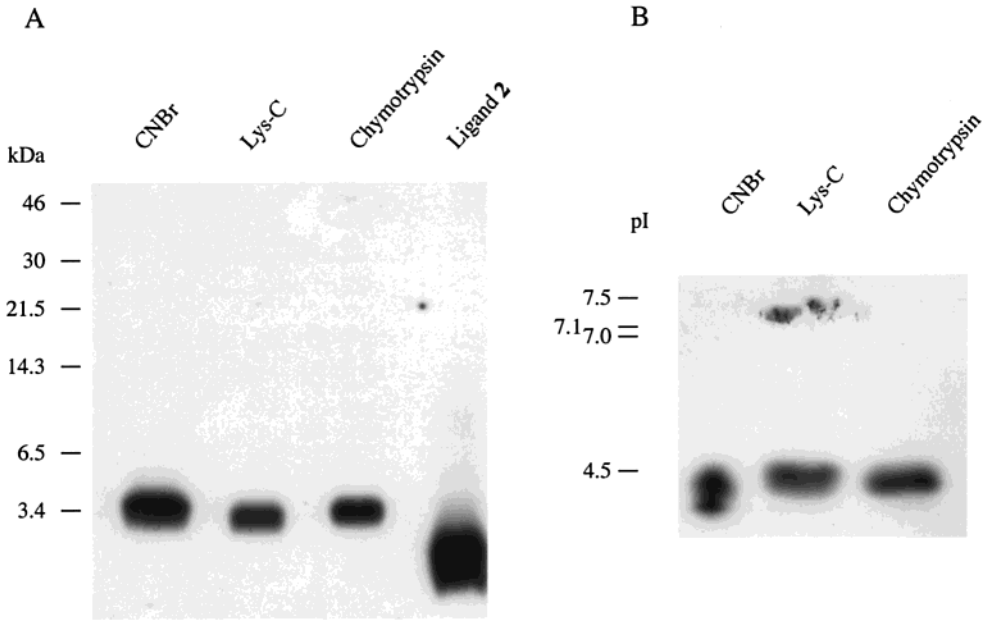

FIGURE 5: Autoradiographs of digestions of the β_3−**2** photoconjugate by CNBr, Lys-C, and chymotrypsin. (A) Samples were analyzed by 16.5% w/v Tricine/SDS−PAGE. Radiograph is a representative of at least three reproducible independent experiments. The nonconjugated ligand **2** (MW = 1531) is shown for comparison. Molecular weight markers are shown on the left side of the autoradiograph. B) Isoelectric focusing gel analysis at pH gradient 3−10. Colored IEF protein standards are shown on the left side of the autoradiograph. Radiographs are representative of at least three reproducible independent experiments.

lies within the sequence β_3[130−171]. This fragment has a theoretical molecular mass of 6.3 kDa when conjugated to the radioactive ligand. Treatment of the BNPS-Skatole-generated band with Glu-C yielded a new radioactive band with gel mobility corresponding to this molecular weight (Figure 3, lane 6), substantiating the identification of β_3[130−171] as the segment containing the putative site of cross-linking for ligand **2**.

To further delineate the cross-linking site, three additional cleavage agents were applied: CNBr, which cleaves specifically at the C-terminus of methionine residues, endoproteinase Lys-C, which cleaves C-terminally to lysine residues, and chymotrypsin, which cleaves C-terminally to aromatic residues. The apparent molecular masses of the conjugated fragments generated by these cleavage agents were all in the molecular mass range of 2.5−4.5 kDa (Figure 5A). The resolution offered by the SDS−PAGE analysis (16.5% gel, tricine buffer system) was not sufficient to determine accurately the masses of the conjugated fragments generated by CNBr, Lys-C, and chymotrypsin. Since each of these cleavage agents produces several putative fragments within this molecular weight range, all overlapping with the region β_3[130−171] (Figure 4A), the identity of the conjugated fragment could not be unambiguously determined using electrophoretic mobility in SDS−PAGE. Attempts to use higher resolution gels, i.e., with increased concentrations of acrylamide or bis-acrylamide or with the addition of urea or 10−20% gradient gels still failed to provide sufficient resolving power.

Despite recent advances in mass spectrometry techniques, sequencing of minute amounts of membrane-embedded receptor fragments is still a considerable challenge. Thus, all of our attempts to achieve this goal using our in-house SMART micropurification HPLC system and Micromass Platform LCZ4000 electrospray ionization mass spectrometer could not be successfully accomplished. No signal could be detected even by a highly sensitive Vision 2000 (Finnigan) MALDI-TOF mass spectrometer equipped with a nitrogen laser (Roche Pharma AG, Switzerland). Therefore, to further localize the cross-linking site a different biochemical approach was pursued. The CNBr-, Lys-C-, and chymotrypsin-generated bands were excised and electroeluted from the original gels, treated extensively to remove any remaining SDS (see experimental procedures), and analyzed by isoelectric focusing (IEF). The predicted isoelectric point (p*I*) values of the putative CNBr-, Lys-C-, and chymotrypsin-generated conjugated fragments, overlapping with the sequence β_3[130−171], are shown in Figure 4B. This orthogonal analysis offers the resolution required to identify unambiguously the conjugated fragment produced by each of the three cleavage agents. As shown in Figure 5B, the conjugated fragments from all three digestion pathways migrated according to an apparent p*I* value of ∼4. The only possible overlapping fragments with both the observed molecular mass and pI values are the CNBr-generated fragment β_3[166−180] (molecular mass = 3.6 kDa, p*I* = 3.66), the Lys-C-generated fragment β_3[160−181] (molecular mass = 4.4 kDa, p*I* = 4.09), and the chymotrypsin-generated fragment β_3[167−178] (molecular mass = 3.1 kDa, p*I* = 3.88) (Figure 4B).

Combining these results with the fragmentation patterns observed for BNPS-Skatole and Glu-C, we conclude that the overlapping 5-amino acid sequence $I^{167}SPPE^{171}$ of the β_3 chain represents a minimal chymotrypsin- and Glu-C-cleavage-restricted domain that includes the photoinsertion site for the N-terminally located Bp in photoligand **2**.

Molecular Modeling. The molecular model for the β_3[99−300] domain developed here assumes the existence of an I-like domain fold in the conserved region of β_3 and the sequence homology shown in Figure 1. The presence of disulfide bonds between cysteines 177−184 and 232−273 is also assumed in the model. The model differs from that

proposed by Tozer and co-workers (*21*), which is based on homology with the α_M-I-domain. The difference arises from the large gap (over 10 residues) located at residue 210 of β_3 in the sequence homology used by Tozer et al., which is not present in the homology used here. It is important to point out that this difference is C-terminal to the region of β_3 demonstrated to interact with the RGD-containing peptide ligand.

DISCUSSION

Photoaffinity cross-linking has been recognized increasingly as an attractive methodology for structural studies of complex protein systems (*75*, *76*). This methodology has the potential to enable mapping of the interface between receptor and ligand, which subsequently can be used to create a three-dimensional model of the bimolecular complex, as has been recently demonstrated for cholecystokinin (*77*, *78*), parathyroid hormone (*71*, *79*), and vasopressin (*80*). This approach holds the promise of providing useful insights in the integrin field, which presents the additional complexity of heterodimeric receptors. Previous cross-linking studies of integrins with RGD-based ligands identified relatively large domains (*36*, *38*, *39*, *81*) that are only of limited use as constraints for building a ligand−receptor model.

The contact site identified in this report is for the photophore positioned N-terminal to the RGD triad (ligand **2**); this site has been delimited to a five-amino acid domain. It is located ~60 residues C-terminal to the contact domain reported for a closely similar analogue containing the same photophore positioned C-terminal to the RGD motif (ligand **1**) (*42*). Both of these contact sites are within the large cross-linking domain β_3[61−203] previously identified by Smith et al. (*38*). The higher resolution achieved in the current study enables for the first time the assignment of the topological orientation of the RGD binding site within the β_3 subunit.

A detailed structural model describing integrin−ligand interaction is highly sought (*82*, *83*). In the absence of high-resolution structural data for integrin β-subunits, the prevailing model consists of two major, homology-derived structural elements: (i) a conserved ~200-amino acid domain at the N-terminal region, homologous to the vWF A-domain and to the I-domains found in integrin α-subunits, termed the I-like domain (*51*, *52*, *82*) and (ii) a MIDAS-like motif, homologous to the MIDAS motif found in I-domains. The prediction of the presence of this latter motif is based on the observation that the DXSXS sequence, common to all I-domains, is also present in all integrin β-subunits (*17*, *18*, *45*). As mentioned above, it has been demonstrated that I-domains contain the major ligand-binding site in those integrins that contain this domain. Since not all α-subunits contain an I-domain, but all β subunits are predicted to contain an I-like domain, it is expected that in integrins that do not contain an I-domain, binding of the ligand occurs predominantly at the I-like domain of the β-subunit. In the β_3 subunit, the I-like domain has been predicted (by homology modeling) to span residues 90−328 (*84*), 110−294 (*21*), or 107−292 (*85*).

Many studies have shown that the MIDAS motif, particularly residues in the DXSXS region, is essential for ligand binding (*17*, *18*, *21*, *29*, *85*). Intriguingly, homology modeling of the putative I-like domain region in the β_3 subunit (based on the crystal structure of the α_M-I-domain) yielded contradictory conclusions. Tozer et al. (*21*) and Lin et al. (*85*) both find a crucial role for the MIDAS-like motif of the β_3 subunit in ligand binding. However, while the former study suggests that the conserved region of β_3 adopts the I-like domain fold, the latter, using the same crystal structure as a modeling template, implies that it does not.

Our cross-linking data are not consistent with the coexistence of both an I-like domain in the conserved region of the β_3 subunit and proximity between the RGD-binding site and the MIDAS-like motif. Our models of the β_3-I-like domain use the α_M-, α_L-, or α_2-I-domain as templates. While the resolution of these experimentally based models cannot provide the exact location of the RGD-binding site, the constraints obtained through the cross-linking experiments localize the binding site at the opposite side (nadir) of the putative I-like domain relative to the MIDAS-like motif (Figure 6).

Two mutually exclusive hypotheses may be conceived that explain our observations: (i) the protein fold of the conserved region of the β_3 subunit is substantially different from the typical dinucleotide-binding structure found for I-domains, i.e., the conserved region does not adopt an I-like domain structure or (ii) the conserved region of the β_3 subunit does adopt an I-like domain structure, but the metal and ligand binding sites are located at distinct sites on opposite sides of the module. If the first hypothesis is correct, then the RGD-binding site and the MIDAS-like motif (or parts of it) could still be proximal in space and enable direct, or very close, interaction between ligand and metal in the bound state. As mentioned before, ambiguity exists with respect to the validity of the I-like domain homology-based model (*21*, *85*), and this question awaits further elucidation. However, if the second hypothesis appears to be true and the region β_3[99−300] does adopt an I-like domain structure (Figure 6), our cross-linking data indicate that interaction between the RGD motif and the metal ion is not feasible. Importantly, unlike previous studies that are based on indirect observations and, of necessity, make inferential conclusions, our results are based on direct formation of a specific covalent bond between the ligand and a unique site in the integrin, which is identified by biochemical methods. The covalent attachment we observe is reproducible, occurs when the ligand−integrin complex is in equilibrium, is dependent upon the presence of Ca^{2+} and Mg^{2+} ions (data not shown), and is competitively inhibited by the nonmodified parent peptide in a dose-dependent manner. It is therefore likely to represent an authentic site of contact at the ligand−integrin interface.

The previously identified contact domain, β_3[99−118] (*42*), is located at the very N-terminus of the putative I-like domain (Figure 6). This region was predicted to adopt a β-strand−coil−β-strand conformation (*84*). Our model, based in this region on the vWF A1-domain, is in agreement with this prediction. The second putative β-strand corresponds to strand A of the I-like domain. The loop preceding this strand is close in space to the second contact site, β_3[167−171]. Strand A of the putative I-like domain leads from the nadir to the apex of the module, where it is immediately followed by the DXSXS metal-binding sequence (Figure 6). However, according to our model, strand A is not accessible for contact with the ligand. The model suggests that the C-terminal side of the RGD motif interacts either with the first putative

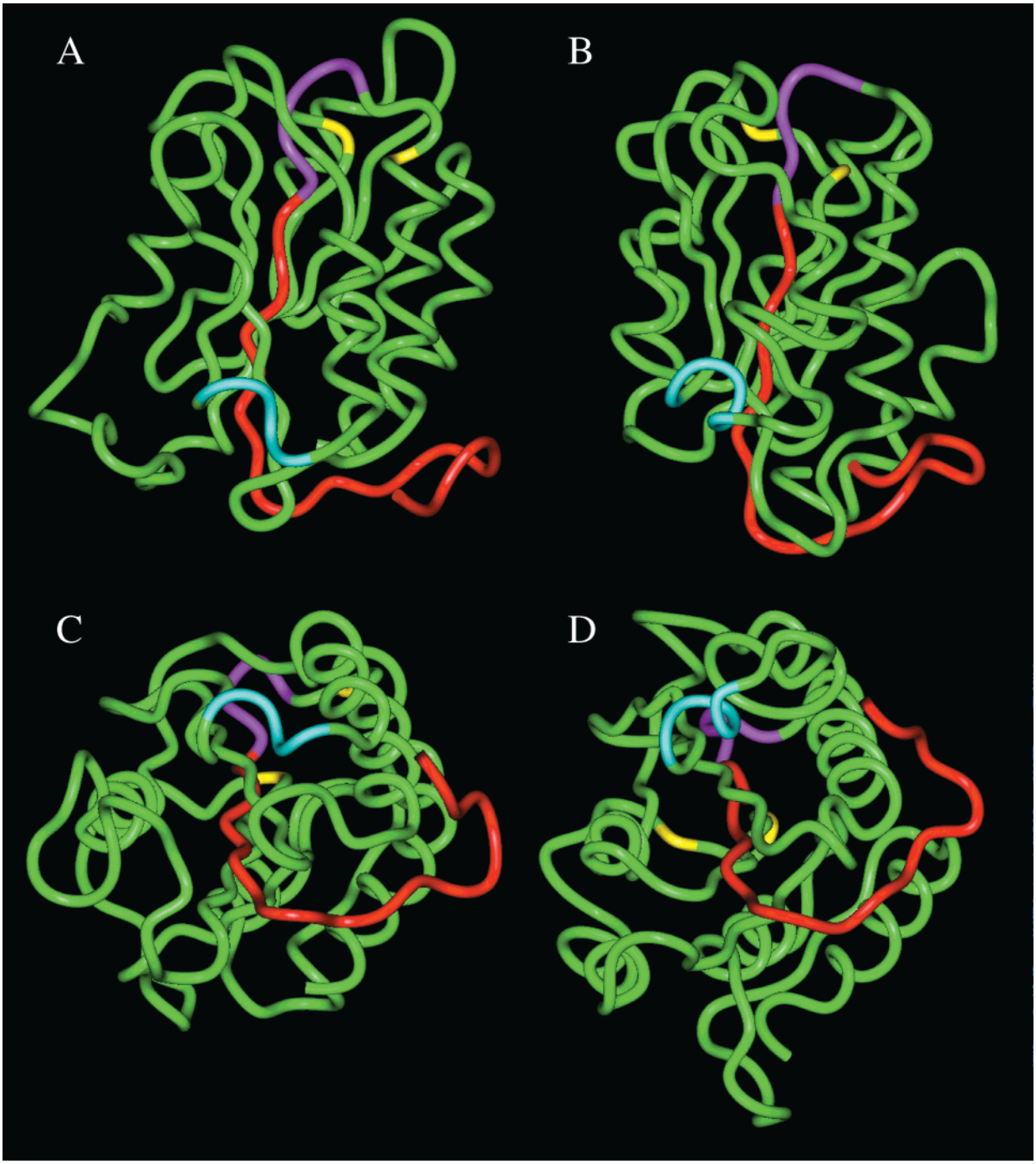

FIGURE 6: Three-dimensional models of the N-terminal conserved domain, β_3[99−300], folded into an I-like domain structure. Panels A and B, side view. Panels C and D, bottom view. The left-hand side model is based on the crystal structure of the α_2-I-domain (A and C). The right-hand side model based on α_M-I-domain (B and D) and is adopted from Tozer et al. (*21*). The cross-linking sites identified in the current and previous (*42*) studies are highlighted in blue and red, respectively. The $D^{119}YSLS^{123}$ motif is highlighted in magenta, and the other residues participating in the MIDAS motif are in yellow. These residues are D113 and T232 in the α_2-based model, and D217 and E220 in the α_M-based model (*21*).

β-strand or with the middle loop in the β_3[99−118] region. Interaction with strand A would require a major conformational rearrangement to take place upon binding of the ligand. Although it is clear that ligand binding confers conformational changes that subsequently lead to integrin activation and/or signal transduction, there are no data supporting a profound rearrangement that would bring two parts of the module, initially far apart from each other, such as the MIDAS-like motif and the cross-linking site, β_3[167−171], into proximity.

A small domain, β_3[177−183], proximal to the newly identified contact site, β_3[167−171], has been shown previously to play a role in dictating ligand specificity (*23*). Recently, Oxvig et al. reported that residues in a region of the α_M-I-domain homologous to β_3[177−183], together with residues near the DXSXS sequence, comprise the binding site for mAb CBRM1/5, which recognizes an activated form of the module (*86*). These observations support an important role for cooperativity between the MIDAS-like motif and the newly identified β_3[167−171] domain in ligand binding

but do not necessarily implicate proximity between the two regions.

On the basis of the crystal structure of the I-domain of the α_L-subunit, it has been suggested that the divalent cation-dependence of ligand binding arises either because of direct interactions between the ligand and the metal or because the metal is required to promote a favorable quaternary arrangement of the integrin (*47*). In the case of the α_2-I-domain, the former hypothesis proved to be correct (*50*), yet it is not clear whether this is true for the putative I-like domains. Although our cross-linking data cannot unequivocally rule out this possibility for the β_3 subunit, they suggest that the hypothesis of direct interaction between the RGD sequence and the metal cation or the MIDAS-like motif (*55*, *87*) is improbable. In future studies, it may be possible to position a photoreactive group closer to or even within the RGD triad and thereby obtain a more conclusive answer to this question.

Recent success in expression of functional soluble truncated forms of integrins (*28*, *88*, *89*) and of a β_3 fragment (*90*) may provide an opportunity to study the three-dimensional structures of these proteins in detail by X-ray crystallography and/or NMR. Combined with our efforts toward detailed mapping of the integrin−ligand interface, the structural data from these different lines of investigation should provide a comprehensive basis for building a detailed experimentally derived integrin−ligand complex model.

In summary, we present in this work a second step toward systematic mapping of the bimolecular interface between the β_3 binding site of integrin $\alpha_V\beta_3$ and the cyclic RGD-containing peptide ligands. Combining information regarding the newly identified contact site, β_3[167−171], and the previously identified contact site β_3[99−118], we conclude that the model that assumes both the presence of an I-like domain fold for the conserved N-terminal region of the β_3 subunit and proximity between ligand- and metal-binding sites in the ligand-bound conformation is unlikely. Unless substantial conformational rearrangements take place, which alter the I-domain-like structure and bring the RGD and the MIDAS-like motif close together after ligand binding, coexistence of the two components of the model is not supported by our data.

REFERENCES

1. Clark, E. A., and Brugge, J. S. (1995) *Science 268*, 233−239.
2. Hynes, R. O. (1992) *Cell 69*, 11−25.
3. Loftus, J. C., Smith, J. W., and Ginsberg, M. H. (1994) *J. Biol. Chem. 269*, 25235−25238.
4. Stuiver, I., and O'Toole, T. E. (1995) *Stem Cells 13*, 250−262.
5. Garratt, A. N., and Humphries, M. J. (1995) *Acta Anat. 154*, 34−45.
6. Ruoslahti, E. (1996) *Annu. Rev. Cell Dev. Biol. 12*, 697−715.
7. Mullen, D. G., Cheng, S., Ahmed, S., Blevitt, J. M., Bonnin, D., Craig, W. S., Ingram, R. T., Mazur, C., Minasyan, R., Tolley, J. O., Tschopp, J. F., and Pierschbacher, M. D. (1996) in *Peptides: Chemistry, Structure and Biology* (Kaumaya, P. T. P., and Hodges, R. S., Eds.) pp 207−208, Mayflower Scientific Ltd, U.K.
8. Haubner, R., Finsinger, D., and Kessler, H. (1997) *Angew. Chem., Int. Ed. Engl. 36*, 1374−1389.
9. Keenan, R. M., Miller, W. H., Kwon, C., Ali, F. E., Callahan, J. F., Calvo, R. R., Hwang, S.-M., Kopple, K. D., Peishoff, C. E., Samanen, J. M., Wong, A. S., Yuan, C.-K., and Huffman, W. F. (1997) *J. Med. Chem. 40*, 2289−2292.
10. Keenan, R. M., Callahan, J. F., Samanen, J. M., Bondinell, W. E., Calvo, R. R., Chen, L., DeBrosse, C., Eggleston, D. S., Haltiwanger, R. C., Hwang, S. M., Jakas, D. R., Ku, T. W., Miller, W. H., Newlander, K. A., Nichols, A., Parker, M. F., Southhall, L. S., Uzinskas, I., Vasko-Moser, J. A., Venslavsky, J. W., Wong, A. S., and Huffman, W. F. (1999) *J. Med. Chem. 42*, 545−559.
11. Helfrich, M. H., Nesbitt, S. A., Dorey, E. L., and Horton, M. A. (1992) *J. Bone Miner. Res. 7*, 335−343.
12. Engleman, V. W., Nickols, G. A., Ross, F. P., Horton, M. A., Griggs, D. W., Settle, S. L., Ruminski, P. G., and Teitelbaum, S. L. (1997) *J. Clin. Invest. 99*, 2284−2292.
13. Yamamoto, M., Fisher, J. E., Gentile, M., Seedor, J. G., Leu, C.-T., Rodan, S. B., and Rodan, G. A. (1998) *Endocrinology 139*, 1411−1418.
14. Dransfield, I., Cabanas, C., Craig, A., and Hogg, N. (1992) *J. Cell. Biol. 116*, 219−226.
15. Kirchhofer, D., Grzesiak, J., and Pierschbacher, M. D. (1991) *J. Biol. Chem. 266*, 4471−4477.
16. Hu, D. D., Barbas, C. F., and Smith, J. W. (1996) *J. Biol. Chem. 271*, 21745−21751.
17. Loftus, J. C., O'Toole, T. E., Plow, E. F., Glass, A., III, A. L. F., and Ginsberg, M. H. (1990) *Science 249*, 915−918.
18. Bajt, M. L., and Loftus, J. C. (1994) *J. Biol. Chem. 269*, 20913−20919.
19. McGuire, S. L., and Bajt, M. L. (1995) *J. Biol. Chem. 270*, 25866−25871.
20. Ma, L., Conrad, P. J., Webb, D. L., and Blue, M. L. (1995) *J. Biol. Chem. 270*, 18401−18407.
21. Tozer, E. C., Liddington, R. C., Sutcliffe, M. J., Smeeton, A. H., and Loftus, J. C. (1996) *Cell 79*, 659−667.
22. Tozer, E. C., Baker, E. K., Ginsberg, M. H., and Loftus, J. C. (1999) *Blood 93*, 918−924.
23. Takagi, J., Kamata, T., Meredith, J., Puzon-McLaughlin, W., and Takada, Y. (1997) *J. Biol. Chem. 272*, 19794−19800.
24. Lin, E. C. K., Ratnikov, B. I., Tsai, P. M., Carron, C. P., Myers, D. M., Barbas, C. F., III, and Smith, J. W. (1997) *J. Biol. Chem. 272*, 23912−23920.
25. Douglass, W. A., Hyland, R. H., Buckley, C. D., Al-Shamkhani, A., Shaw, J. M., Scarth, S. L., Simmons, D. L., and Law, S. K. (1998) *FEBS Lett. 440*, 414−418.
26. Cao, Z., Huang, K., and Horwitz, A. F. (1998) *J. Biol. Chem. 273*, 31670−31679.
27. Ferrer, M., Tao, J., Iruin, G., Sanchez-Ayuso, M., Gonzalez-Rodriguez, J., Parrila, J., and Gonzalez-Manchon, C. (1998) *Blood 92*, 4712−4720.
28. Peterson, J. A., Visentin, G. P., Newman, P. J., and Aster, R. H. (1998) *Blood 92*, 2053−2063.
29. D'Souza, S. E., Haas, T. A., Piotrowicz, R. S., Byers-Ward, V., McGrath, D. E., Soule, H. R., Cierniewski, C., Plow, E. F., and Smith, J. W. (1994) *Cell 79*, 659−667.
30. Buttery, P. C., Mallawaarachchi, C. M., Milner, R., Doherty, P., and French-Constant, C. (1999) *Biochem. Biophys. Res. Commun. 259*, 121−127.
31. Pelletier, A. J., Kunicki, T., and Quaranta, V. (1996) *J. Biol. Chem. 271*, 1364−1370.
32. Honda, S., Tomiyama, Y., Pelletier, A. J., Annis, D., Honda, Y., Orchekowski, R., Ruggeri, Z., and Kunicki, T. J. (1995) *J. Biol. Chem. 270*, 11947−11954.
33. Barbas, C. F., Languino, L. R., and Smith, J. W. (1993) *Proc. Natl. Acad. Sci. U.S.A. 90*, 10003−10007.
34. Yano, S., Suzuki, K., Katoh, M., Sagita, Y., Kaku, S., Kawamura, K., and Masuho, Y. (1994) *J. Biochem. (Tokyo) 116*, 778−786.
35. Kamata, T., Puzon, W., and Takada, Y. (1995) *Biochem. J. 305*, 945−951.
36. D'Souza, S. E., Ginsberg, M. H., Burke, T. A., Lam, S. C.-T., and Plow, E. F. (1988) *Science 242*, 91−93.
37. D'Souza, S. E., Ginsberg, M. H., Burke, T. A., and Plow, E. F. (1990) *J. Biol. Chem. 265*, 3440−3446.
38. Smith, J. W., and Cheresh, D. A. (1988) *J. Biol. Chem. 263*, 18726−18731.
39. Smith, J. W., and Cheresh, D. A. (1990) *J. Biol. Chem. 265*, 2168−2172.

40. Calvete, J. J., Henschen, A., and Gonzalez-Rodriguez, J. (1991) *Biochem. J. 274*, 63−71.
41. Chen, L. L., Lobb, R. R., Cuervo, J. H., Lin, K.-C., Adams, S. P., and Pepinsky, R. B. (1998) *Biochemistry 57*, 8745−8755.
42. Bitan, G., Scheibler, L., Rosenblatt, M., and Chorev, M. (1999) *Biochemistry 38*, 3414−3420.
43. Emsley, J., King, S. L., Bergelson, J. M., and Liddington, R. C. (1997) *J. Biol. Chem. 272*, 28512−28517.
44. Qu, A., and Leahy, D. J. (1995) *Proc. Natl. Acad. Sci. U.S.A. 92*, 10277−10281.
45. Lee, J.-O., Rieu, P., Arnaout, M. A., and Liddington, R. (1995) *Cell 80*, 631−638.
46. Nolte, M., Pepinsky, R. B., Venyaminov, S. Y., Koteliansky, V., Gotwals, P. J., and Karpusas, M. (1999) *FEBS Lett. 452*, 379−385.
47. Qu, A., and Leehy, D. J. (1996) *Structure 4*, 931−942.
48. Lee, J. O., Bankson, L. A., Arnaout, M. A., and Liddington, R. C. (1995) *Structure 3*, 1333−1340.
49. Salminen, T. A., Nymalm, Y., Kankare, J., Kapyla, J., Heino, J., and Johnson, M. S. (1999) *Acta Crystallogr. D Biol. Crystallogr. 55*, 1365−1367.
50. Emsley, J., Knight, C. G., Farndale, R. W., Barnes, M. J., and Liddington, R. C. (2000) *Cell 100*, 47−56.
51. Tuckwell, D. S., and Humphries, M. J. (1997) *FEBS Lett. 400*, 297−303.
52. Takada, Y., Kamata, T., Irie, A., Puzon-McLaughlin, W., and Zhang, X. P. (1997) *Matrix Biol. 16*, 143−151.
53. Springer, T. A. (1997) *Proc. Natl. Acad. Sci. U.S.A. 94*, 65−72.
54. Bork, P., Doerks, T., Springer, T., and Snel, B. (1999) *Trends Biochem. Sci. 24*, 261−263.
55. Dickeson, S. K., and Santoro, S. A. (1998) *Cell. Mol. Life Sci. 54*, 556−566.
56. Smith, J. W., and Cheresh, D. A. (1991) *J. Biol. Chem. 266*, 11429−11432.
57. Hantgan, R. R., Paumi, C., Rocco, M., and Weisel, J. W. (1999) *Biochemistry 38*, 14461−14474.
58. Horton, M. A. (1997) *Int. J. Biochem. Cell Biol. 29*, 721−725.
59. Brooks, P. C., Strömblad, S., Sanders, L. C., von Schalscha, T. L., Aimes, R. T., Stetler-Stevenson, W. G., Quigly, J. P., and Cheresh, D. A. (1996) *Cell 85*, 683−693.
60. Healy, D. L., Rogers, P. A., Hii, L., and Wingfield, M. (1998) *Hum. Reprod. Update 4*, 736−740.
61. Penta, K., Varner, J. A., Liaw, L., Hidai, C., Schtzman, R., and Quertermous, T. (1999) *J. Biol. Chem. 274*, 11101−11109.
62. Varner, J. A., and Cheresh, D. A. (1996) *Curr. Opin. Cell. Biol. 8*, 724−730.
63. Uhm, J. H., Dooley, N. P., Kyritsis, A. P., Rao, J. S., and Gladson, C. L. (1999) *Clin. Cancer Res. 5*, 1587−1594.
64. Cripps, B. A., Engleman, V. W., Settle, S. L., Delarco, J., Ornberg, R. L., Helfrich, M. H., Horton, M. A., and Nickols, G. A. (1996) *Endocrinology 137*, 918−924.
65. Boissy, P., Machuca, I., Pfaff, M., Ficheux, D., and Jurdic, P. (1998) *J. Cell. Sci. 111*, 2563−2574.
66. Rodan, S. B., and Rodan, G. A. (1997) *J. Endocrinol. 154* Suppl., S47−S56.
67. Carron, C. P., Meyer, D. M., Pegg, J. A., Engleman, V. W., Nickols, M. A., Settle, S. L., Westlin, W. F., Ruminski, P. G., and Nickols, G. A. (1998) *Cancer Res. 58*, 1930−1935.
68. Bitan, G., Scheibler, L., Teng, H., Rosenblatt, M., and Chorev, M. (2000) *J. Pept. Res. 55*, 181−194.
69. Greenberg, Z., Stoch, S. A., Traianedes, K., Teng, H., Suva, L. J., Rosenblatt, M., and Chorev, M. (1999) *Anal. Biochem. 266*, 153−164.
70. Bolton, A. E., and Hunter, W. M. (1972) *J. Endocrinol. 55*, xxx-xxxi.
71. Bisello, A., Mierke, D. F., Pellegrini, M., Rosenblatt, M., Suva, L. J., and Chorev, M. (1998) *J. Biol. Chem. 273*, 22498−22505.
72. Miller, D. W., and Elgin, S. C. R. (1974) *Anal. Biochem. 60*, 142−148.
73. Emsley, J., Cruz, M., Handin, R., and Liddington, R. (1998) *J. Biol. Chem. 273*, 10396−10401.
74. Fitzgerald, L. A., Steiner, B., Jr., S. C. R., Lo, S. S., and Phillips, D. R. (1987) *J. Biol. Chem. 262*, 3936−3937.
75. Prestwich, G. D., Dorman, G., Elliott, J. T., Marecak, D. M., and Chaudhary, A. (1997) *Photochem. Photobiol. 65*, 222−234.
76. Knorre, D. G., and Godovikova, T. S. (1998) *FEBS Lett. 433*, 9−14.
77. Ji, Z. S., Hadac, E. M., Henne, R. M., Patel, S. A., Lybrand, T. P., and Miller, L. J. (1997) *J. Biol. Chem. 272*, 24393−24401.
78. Hadac, E. M., Ji, Z., Pinon, D. I., Henne, R. M., Lybrand, T. P., and Miller, L. M. (1999) *J. Med. Chem. 42*, 2105−2111.
79. Rölz, C., Pellegrini, M., and Mierke, D. F. (1999) *Biochemistry 38*, 6397−6405.
80. Phalipou, S., Seyer, R., Cotte, N., Breton, C., Barberis, C., Hibert, M., and Mouillac, B. (1999) *J. Biol. Chem. 274*, 23316−23327.
81. Calvete, J. J., McLane, M. A., Stewart, G. J., and Niewiarowski, S. (1994) *Biochem. Biophys. Res. Commun. 202*, 135−140.
82. Humphries, M. J. (1999) *Biochem. Soc. Symp. 65*, 63−78.
83. Tuckwell, D. S., Humphries, M. J., and Brass, A. (1994) *Cell Adhes. Commun. 2*, 385−402.
84. Puzon-McLaughlin, W., and Takada, Y. (1996) *J. Biol. Chem. 271*, 20438−20443.
85. Lin, E. C. K., Ratnikov, B. I., Tsai, P. M., Gonzalez, E. R., McDonald, S., Pelletier, A. J., and Smith, J. W. (1997) *J. Biol. Chem. 272*, 14236−14243.
86. Oxvig, C., Lu, C., and Springer, T. A. (1999) *Proc. Natl. Acad. Sci. U.S.A. 96*, 2215−2220.
87. Bergelson, J. M., and Hemler, M. E. (1995) *Curr. Biol. 5*, 615−617.
88. Wippler, J., Konus, W. C., Schlaeger, E. J., Kuhn, H., Hadvary, P., and Steiner, B. (1994) *J. Biol. Chem. 269*, 8754−8761.
89. Mehta, R. J., Diefenbach, B., Brown, A., Cullen, E., Jonczyk, A., Gussow, D., Luckenbach, G. A., and Goodman, S. L. (1998) *Biochem. J. 330*, 861−869.
90. Cierniewski, C. S., Byzova, T., Papierak, M., Haas, T. A., Niewarowska, J., Zhang, L., Cieslak, M., and Plow, E. F. (1999) *J. Biol. Chem. 274*, 16923−16932.

BI000877A